# Heat-fraction-limited CW Yb:YAG cryogenic solid-state laser with 100% photon slope efficiency

**David C. Brown*, Thomas M. Bruno, and Joseph M. Singley**

*Snake Creek Lasers, LLC, Hallstead, PA, 18822, USA*
**dbrown@snakecreeklasers.com*

**Abstract:** We report the demonstration of a heat-fraction-limited CW Yb:YAG laser operating near 77 K with output at 1029 nm, pumped with a diffraction-limited room-temperature CW Nd:YAG laser operating at 946 nm. With a 50% reflectivity outcoupler, the average threshold absorbed pump power was 18.8 mW and the average slope efficiency 91.9%, close to the heat-fraction limited value of 91.5%. Average optical to optical and photon slope efficiencies are 84% and 100% respectively. To the best of our knowledge this solid-state laser is the first to operate at the heat-fraction-limit and demonstrates record slope, photon slope and optical-optical efficiencies for optically-pumped solid-state lasers.



**OCIS codes:** (140.3460) Lasers: (140.0140) Lasers and laser optics; (140.3580) Lasers, solid state; (140.3615) Lasers, ytterbium

## References and links

1. D. C. Brown, ""The promise of cryogenic lasers," Invited Paper, IEEE Special Issue on Tops," Quantum Electron. **11**, 587–599 (2005).
2. T. Y. Fan, D. J. Ripin, R. L. Aggarwal, J. R. Ochoa, B. Chann, M. Tilleman, and J. Spitzberg, ""Cryogenic $Yb^{3+}$-doped solid-state lasers", Invited Paper," IEEE J. Sel. Top. Quantum Electron. **13**(3), 448–459 (2007).
3. P. Lacovara, H. K. Choi, C. A. Wang, R. L. Aggarwal, and T. Y. Fan, "Room-temperature diode-pumped Yb:YAG laser," Opt. Lett. **16**(14), 1089–1091 (1991).
4. D. J. Ripin, J. R. Ochoa, R. L. Aggarwal, and T. Y. Fan, "165-W cryogenically cooled Yb:YAG laser," Opt. Lett. **29**(18), 2154–2156 (2004).
5. T. Shoji, S. Tokita, J. Kawanaka, M. Fujita, and Y. Izawa, "Quantum-defect-limited operation of diode-pumped Yb:YAG laser at low temperature," Jpn. J. Appl. Phys. **43**(No. 4A), L496–L498 (2004).
6. S. Tokita, J. Kawanaka, M. Fujita, T. Kawashima, and Y. Izawa, "Sapphire-conductive end-cooling of high power cryogenic Yb:YAG lasers," Appl. Phys. B **80**(6), 635–638 (2005).
7. D. C. Brown, J. M. Singley, E. Yager, J. W. Kuper, B. J. Lotito, and L. L. Bennett, "Innovative high-power CW Yb:YAG cryogenic laser," Proc. SPIE **6552**, 65520D (2007).
8. D. C. Brown, J. M. Singley, E. Yager, K. Kowalewski, J. Guelzow, and J. W. Kuper, "Kilowatt class high-power CW Yb:YAG cryogenic laser," Proc. SPIE **6952**, 69520K (2008).
9. D. C. Brown and V. Vitali, "Yb:YAG Kinetics model including saturation and power conservation," paper accepted for publication in IEEE J. Quantum. Electron., July (2010).
10. D. C. Brown, R. L. Cone, Y. Sun, and R. W. Equal, "Yb:YAG Absorption at ambient and cryogenic temperatures," IEEE J. Sel. Top. Quantum Electron. **11**(3), 604–612 (2005).
11. D. C. Brown, V. Vitali, and T. M. Bruno, "Saturated absorption effects in CW-pumped solid-state lasers," paper accepted for publication in IEEE J. Quantum. Electron., July (2010).
12. P. Lacovara, "Energy transfer and up-conversion in Yb:YAG and Yb:Er:YAG," Ph.D. Thesis, Boston University (1992), Available from University Microfilms Inc., Ann Arbor, MI, USA.
13. J. Dong, M. Bass, Y. Mao, P. Deng, and F. Gan, "Dependence of the $Yb^{3+}$ emission cross-section and lifetime on temperature and concentration in yttrium aluminum garnet," J. Opt. Soc. Am. B **20**(9), 1975–1979 (2003).

## 1. Introduction

Significant advances in cryogenically-cooled lasers have made in the past decade. The benefits of cryogenic cooling to significantly reduce, or render thermally induced phase aberrations, stresses, and birefringence insignificant, in solid-state lasers have been examined

#129483 - $15.00 USD Received 2 Jun 2010; revised 15 Jul 2010; accepted 16 Jul 2010; published 22 Jul 2010

in detail in recent papers [1,2]. In addition to the substantial materials properties benefits, cryogenic cooling can also lead to favorable changes in laser properties. For Yb:YAG lasers, for example, the quasi-three-level nature of Yb at room temperature becomes almost purely four-level at 77 K, eliminating ground state absorption. The stimulated-emission cross-section of Yb:YAG increases by almost a factor of five at 77 K, while the saturation intensity is reduced likewise. Yb:YAG is an almost ideal laser system at 77 K, and displays no up-conversion, concentration-quenching, or other deleterious energy transfer mechanisms.

Table 1 below shows a comparison of recent results obtained for Yb:YAG CW lasers operating at or near 77 K [3–8]. As development has progressed, the average power of Yb:YAG cryogenic lasers has risen; References [4–6] have achieved the highest slope efficiencies to date, while Ref [4]. achieved the highest optical-optical efficiency. All of the slope and optical-optical efficiencies are with respect to absorbed pump power, with the exception of Ref [5]. where the method used to calculate slope efficiency is not clear.

**Table 1. Comparison of Recent Cryogenic and Room Temperature Yb:YAG Laser Results**

| Reference | Temperature (K) | Slope Efficiency (With Respect to Absorbed Pump Power) | Optical-Optical Efficiency | Output Power (W) |
|---|---|---|---|---|
| [3] | 77 | 67 | 62 | 0.073 |
| [4] | 77 | 85 | 76 | 165.000 |
| [5] | 77 | 90 | 74 | 0.425 |
| [6] | 77 | 80 | 70 | 75.000 |
| [7] | 77 | 66 | 61 | 264.000 |
| [8] | 77 | 59 | 53 | 550.000 |

In a recent paper produced by our group [9], we have re-examined the heat fraction in Yb:YAG and developed a kinetics model to predict the performance of Yb:YAG lasers operating at 300 and 77 K. The heat fraction for total laser extraction at 77 K is predicted to be 0.085. Pumping is assumed to be at 940 nm. For comparison, the quantum defect value for the heat fraction, again pumping at 940 nm, is 0.086. We have shown [9] that theoretically, the highest slope efficiency for a Yb:YAG laser operating at 77 K is about 90.5% if pumping is at 940 nm. For pumping at 946 nm, as we describe in this paper, the highest efficiency is 91.5%, and we refer to lasers operating with this slope efficiency value as "heat fraction-limited". Table 1 shows that the lasers of Ref's [4,5] have come closest to this condition.

In this paper we describe the design, implementation, and resultant data from a cryogenic Yb:YAG laser operating at 77 K and optically-pumped with a diffraction-limited Nd:YAG laser operating at 946 nm. Section II describes the experimental details, Section III the data and analysis, and in Section IV we discuss the results and conclusions.

## 2. Experimental details

Figure 1 shows the experimental set up. An 808 nm diode-pumped Nd:YAG solid-state laser was built that produces 450 mW of output power at 946 nm. The measured beam-quality of this laser was $M^2 = 1.0 \pm 0.1$. The output $1/e^2$ beam diameter of 150 μm was collimated using a 50 cm focal length lens (L1), and focused into the Yb:YAG crystal assembly using either a 7.5 cm or a 10.0 cm focal length lens L2.

#129483 - $15.00 USD Received 2 Jun 2010; revised 15 Jul 2010; accepted 16 Jul 2010; published 22 Jul 2010

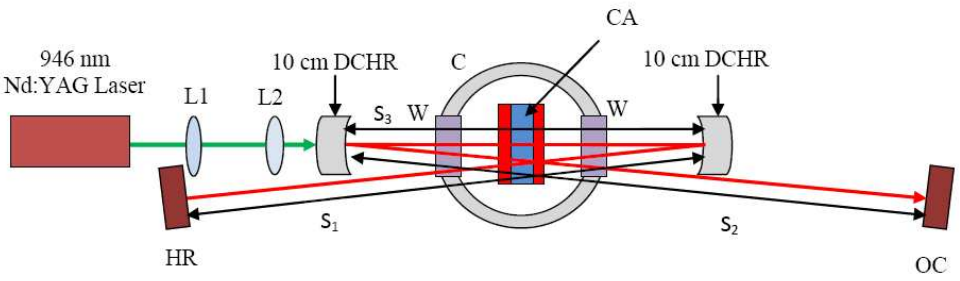


Fig. 1. Experimental set up of 946 nm laser-pumped cryogenic Yb:YAG laser. C-cryogenic liquid nitrogen vacuum dewar, HR- flat high reflector at 1029 nm, OC- curved outcoupler with 50% reflectivity at 1029 nm and 1250 cm radius, W- anti-reflection coated at 1029 nm fused silica windows, 10 cm DCHR- 10 cm radius of curvature, high reflector at 1029 nm, L1- collimating lens, L2- focusing lens, CA- Sapphire-Yb:YAG crystal assembly.

Focusing of the 946 nm pump beam into the Yb:YAG crystal occurs through a 10 cm radius of curvature dichroic mirror whose curved surface is coated to be highly reflective at 1029. The Yb:YAG crystal assembly (CA) employed utilizes a 25 at-% Yb doped disk with a 2 mm thickness and a diameter of 1 cm. The disk is sandwiched between two 1 mm thick, 1 cm diameter C-cut sapphire plates. The Yb:YAG disk is uncoated, as are the inside surfaces of the sapphire disks. The sapphire outer surfaces were anti-reflection coated at 1029 nm and 946 nm. The crystal assembly is cooled by contact of an outer annulus of each of the sapphire disks with an indium annulus which is in turn in contact with a copper heatsink. The copper heatsink is attached to a custom liquid nitrogen cooled vacuum dewar (C) that maintains the crystal assembly near 77 K. The cryogenic dewar uses two 3.2 mm thick fused silica windows to enclose the vacuum; each window was anti-reflection coated on both surfaces at 1029 nm.

In order to produce a small laser beam diameter in the Yb:YAG crystal, we utilized an X-resonator with short radius of curvature mirrors arranged in a near-confocal configuration and long arms. Five sets of data are presented in this article. Sets 1-3 were generated using $S_1 = 64$ cm, $S_2 = 65$ cm, $S_3 \approx 10$ cm, while set 4 used $S_1 = 65$ cm, $S_2 = 64$ cm, $S_3 \approx 10$ cm; all four sets of data used a 7.5 cm focal length lens L2. For data set 5, we used a 10 cm focal length lens L2 and $S_1 = 65$ cm, $S_2 = 64$ cm, $S_3 \approx 10$ cm. Using Paraxia simulations, we have determined that the pump spot $1/e^2$ diameter at the center of the Yb:YAG crystal was about 28 μm using the 7.5 cm focal length lens L2, and about 39 μm using the 10 cm focal length lens. In order to match the pump diameter to the resonator $TEM_{00}$ mode diameter, the resonator was iterated experimentally to maximize the obtained slope efficiency by changing the distance $S_3$.

### 3. Laser data and analysis

We chose to utilize a 946 nm diode-pumped Nd:YAG laser to provide a diffraction-limited pump beam, insuring good overlap with the $TEM_{00}$ resonator mode. While 946 nm is not at the peak of the 940 nm Yb:YAG absorption band [10], calculation shows that about 66.7% small-signal absorption of the pump light can be expected at 77 K. Absorbed pump power was measured by first measuring the transmission of the 946 nm pump light from laser output to that incident on the Yb:YAG crystal as well as the transmission from the Yb:YAG crystal exit face to a calorimeter located outside the resonator. The absorbed power was measured under lasing and non-lasing conditions; for the non-lasing condition, we measured an absorption of 65.2% averaged over all pump data points measured. For the lasing case, we measured an absorption of 62.3%, averaged over all pump data points measured. Since the absorption coefficient decreases as pump intensity increases and increases during lasing conditions, the difference between these two absorption values is attributed in part to the

#129483 - $15.00 USD Received 2 Jun 2010; revised 15 Jul 2010; accepted 16 Jul 2010; published 22 Jul 2010

interplay of those two effects [11] as well as to experimental error. Figure 2 shows the output power as a function of absorbed power for five separate data sets taken with the data taken at different times over a five week period. A complete re-alignment of the laser was performed for each data set. Calibrated stabilized Coherent calorimeters were used for all measurements reported, with accuracies of ± 2%.

In Table 2, we summarize the results for each of the five data sets, listing the threshold absorbed pump power, the slope efficiency, photon slope efficiency, and maximum optical-optical efficiency. The absorbed pump power at threshold was obtained by performing a linear least-squares fit curve to each data set and taking the abscissa intercept; slope efficiency was obtained from the same fit. Photon slope efficiency was obtained by multiplying the slope efficiency by the ratio of the lasing to pump wavelengths, or 1.088. Optical to optical efficiency was determined by taking the maximum optical efficiency corresponding to the maximum pump power, although in two data sets the maximum efficiency occurred below the maximum pump power value. Also shown in Table 2 are the calculated average values and standard deviations for the five data sets. A least-squares linear fit to all data sets, shown in Fig. 2, yields an average slope efficiency of 91.9% and an average threshold power of 18.77 mW. The photon slope efficiency corresponding to the 91.9% slope efficiency is 100%. These values are close to those shown in Table 1 where the average value and standard deviations were calculated from five separate linear fits to the individual data sets.

It is clear from Table 2 that the average (mean) value of the slope efficiencies of 91.9% is very close to the heat-fraction limited value of 91.5% [9], and confirms that within the experimental error (standard deviation) of ± 1.4%, this laser operates very close to the theoretical limit. The same conclusion may be drawn about the photon slope efficiency, which is nearly 100%.

All data sets were taken with the output previously optimized by varying the outcoupler reflectivity, which maximized at 50%. The optical-optical efficiency is plotted in Fig. 3, and reaches an average value of 84.0% at full pump power. The highest optical-optical efficiency recorded was for Data Set 3, almost 86%. This result is substantially greater than the previous measurements summarized in Table 1. All data sets exhibited an optical-optical efficiency greater than 81%. Each data set approaches a peak value as pump power is increased, although the rate at which the peak value is approached is different in each case, a reflection of the degree of overlap of the resonator and pump beams and the ratio of internal resonator intensity to saturation intensity for that particular data set.

**Table 2. Threshold absorbed pump power, slope efficiency, photon slope efficiency, and optical-optical efficiency for all four data sets, with average values and standard deviation.**

| Data Set | Threshold Absorbed Pump Power (mW) | Slope Efficiency (%) | Photon Slope Efficiency (%) | Optical-Optical Efficiency (%) |
|---|---|---|---|---|
| 1 | 19.4 | 90.8 | 98.8 | 85.6 |
| 2 | 20.3 | 92.2 | 100.3 | 81.0 |
| 3 | 11.2 | 92.4 | 100.5 | 85.9 |
| 4 | 21.6 | 90.4 | 98.3 | 83.6 |
| 5 | 21.9 | 93.9 | 102.1 | 83.9 |
| Average Value | 18.9 | 91.9 | 100.0 | 84.0 |
| Standard Deviation | 4.4 | 1.4 | 1.5 | 2.0 |

The data of Fig. 2 display no apparent rolloff dependence on thermal effects. We have verified that for all five data sets reported here, the laser operated at a wavelength of 1029 nm. The output bandwidth (FWHM) was measured for data set 5 with an Ando spectrum analyzer with 0.1 nm resolution to be 0.34 nm, 0.34 nm, and 0.30 nm, corresponding to 33, 96, and 173 mW of output power respectively. The beam-quality has been measured at full power for data set 5 using a Spiricon $M^2$ measurement system, and resulted in $M^2 = 1.1 \pm 0.1$.

#129483 - $15.00 USD Received 2 Jun 2010; revised 15 Jul 2010; accepted 16 Jul 2010; published 22 Jul 2010

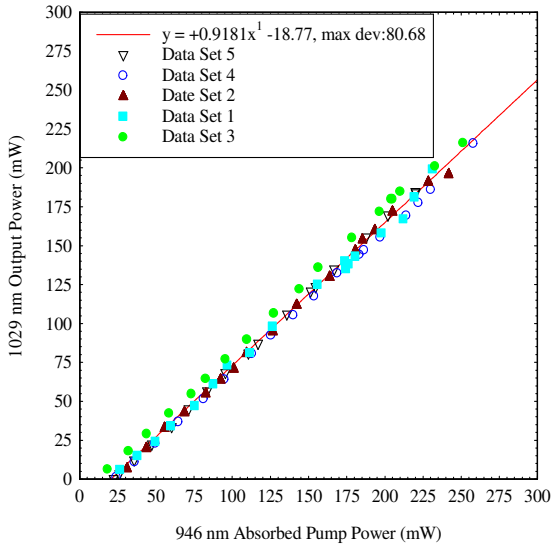


Fig. 2. 1029 nm output power as a function of absorbed 946 nm pump power for four different data sets, using an outcoupler transmission of 50%.

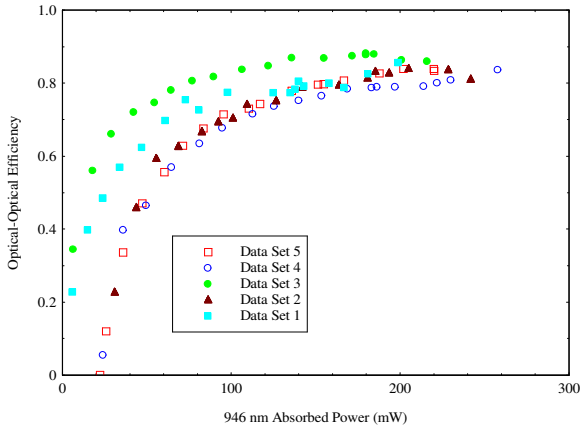


Fig. 3. Optical to optical efficiency as a function of absorbed 946 nm pump power for four different data sets, using an outcoupler transmission of 50%.

### *3.1 Findlay-clay analysis and saturable loss*

We have performed a Findlay-Clay analysis to determine the loss in the resonator. A plot of the absorbed threshold 946 nm pump power is shown in Figure 4 as a function of the parameter -(1/2)ln(R), where R is the outcoupler reflectivity. The R values used in Fig. 4 were measured to be 0.3648, 0.7421, 0.8359, and 0.9619. A linear fit to this data shows that the one-way loss amounts to 22.8%. It is difficult to explain this loss based upon the measured losses in the resonator alone. Taking into account the known reflectivities of the high reflectors in the resonator (99.95% at 1029 nm), the estimated single-pass transmission of the sapphire-Yb:YAG crystal assembly at 77 K (99.45%), and the transmission of the cryogenic dewar windows at 1029 nm (99.42%), we calculate a single-pass loss of only 0.56%. Clearly a 22.8% single-pass loss would cause a significant decrease in the slope efficiency if that loss were operative at the highest pump powers. That the slope efficiency was nevertheless very

#129483 - $15.00 USD Received 2 Jun 2010; revised 15 Jul 2010; accepted 16 Jul 2010; published 22 Jul 2010

high indicates that a saturable loss is operative in this laser. We suspect that the saturable loss is due to parasitic impurity ions present in the laser material acting as non-radiative sinks; these non-radiative sites, combined with the long fluorescence lifetime of Yb:YAG [2], reduce the quantum efficiency of the upper laser level, resulting in an increased heat load, and ultimately leading to ground-state absorption at 1029 nm via increased Boltzmann population of the lower laser level. The role of impurity ions in Yb:YAG has been explored by Locavarra [12]. This parasitic loss is negated as stimulated-emission occurs and becomes less important as the rate of stimulated-emission overwhelms the much slower rate of loss due to the non-radiative sites. A theory exploring this possibility is being developed and will be presented in a future publication.

As pointed out by a reviewer of this article, it is possible that some of the derived 22.8% single-pass loss could have been due to the sensitivity of threshold measurements to resonator alignment. Because we are operating well outside the small output coupling regime (valid for outcoupling transmission values of less than ~ 30%) where the slope efficiency is proportional to T/(T+L) where L is the outcoupler transmission and L the round-trip resonator loss, we cannot at present assess how much of the loss reported here at threshold is due to resonator alignment error and how much is due to a saturable loss, if present.

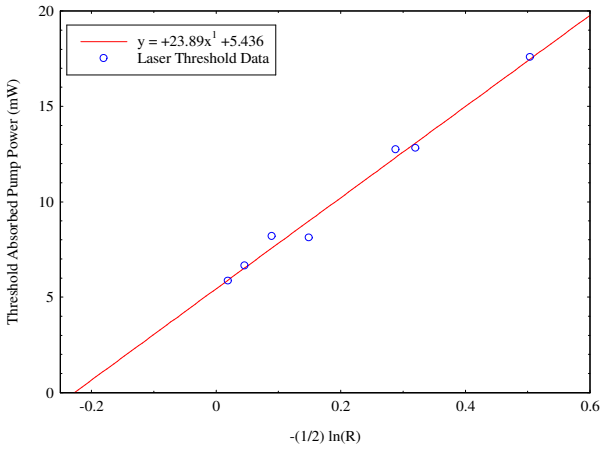


Fig. 4. Findlay-Clay Plot showing threshold absorbed 946 nm pump power as a function of the parameter –(1/2) ln(R), where R is the measured outcoupler reflectivity.

### *3.2 Small-signal gain*

The low average threshold of 18.83 mW of absorbed power using a 50% transmission outcoupler (Table 2) is indicative of a large small-signal gain. If we use the calculated one-way resonator transmission of 0.9903 and an outcoupler reflectivity of 0.5, then we calculate a one-way small-signal gain-length product of 0.351, or an exponential gain of 1.421. If on the other hand we use the Findlay-Clay one-way transmission of 0.54, then we obtain a gain-length product of 0.65, or an exponential gain of 1.92. If we assume the small-signal gain is proportional to the absorbed pump power, and that the Findlay-Clay loss is reduced to the calculated one-way loss of 0.99, then at the maximum absorbed pump power of about 260 mW, the calculated small-signal gain-length product is about 4.9. The corresponding single-pass small-signal exponential gain is then ~127. This high small-signal gain, combined with the low saturation intensity of Yb:YAG at 77 K, ~1.839 kW/cm$^2$ [13], contributes to the high efficiency values reported in this paper.

#129483 - $15.00 USD Received 2 Jun 2010; revised 15 Jul 2010; accepted 16 Jul 2010; published 22 Jul 2010

## 4. Discussion and conclusions

The high slope efficiency achieved with this laser is attributed to a number of factors. To maximize the slope efficiency, the overlap efficiency between the laser and pump beams must be very high and the extraction efficiency must also have a very large value. These two factors, combined with operation at 77 K to minimize thermal effects and maximize the gain, and the fact that Yb:YAG does not exhibit any efficiency robbing parasitic effects such as up-conversion, concentration-quenching, or excited-state absorption, are primarily responsible for the results presented here. Because slope efficiency is defined with respect to the absorbed pump power, the less than ideal absorption of about 62% at 946 nm plays no role. Future iterations of the laser described here will include improving the pump absorption by increasing the optical density of the Yb:YAG crystal and/or multi-passing the pump beam, and by replacing the 946 nm Nd:YAG laser with a high brightness diode laser pump source.

By using an X-resonator operated in the near-confocal regime, a small laser mode diameter is achieved in the Yb:YAG laser crystal, well-matched to the 28-39 μm $1/e^2$ pump diameter. Mode matching between the two beams is achieved in practice by iterating the distance between the center of the curved HR 10 cm radius mirrors and the center of the Yb:YAG crystal. If both the pump and laser beams are completely overlapping spatially (in a 3-D sense), and the laser mode diameter is greater than or equal to the pump beam everywhere in the laser crystal, nearly unity overlap efficiency results. This circumstance is largely attributable to the closeness of the pump and laser wavelengths and to the use of a diffraction-limited pump source rather than a multimode diode source with a large $M^2$.

Calculation shows that inside the Yb:YAG laser crystal and with a 50% transmission outcoupler, the ratio of the peak central intensity of the added forward and backward traveling resonator extraction beams to the saturation intensity is about a factor of 35. This high ratio, which results from the use of a nearly-confocal Z-resonator, when combined with the high small-signal gain, results in near-unity Gaussian beam extraction efficiency [9].

It is clear from the results presented here that the demonstration of heat-fraction-limited, diffraction-limited lasers depends upon a number of important factors, amongst them operation at 77 K to maximize the small-signal gain and eliminate any thermal aberrations, the use of a diffraction-limited pump source whose wavelength is not far different from the laser wavelength to produce a near-unity overlap efficiency, and a small laser mode diameter in the laser crystal to produce a large ratio of laser intensity to saturation intensity. It is hoped that the guidance provided by these principles may lead to other similar demonstrations in the near future.

**Acknowledgement**

The authors thank Victoria Vitali for help with the manuscript and Figures, and the U. S. Army Research Laboratory for support under Contract # W911NF-07-2-0048.

#129483 - $15.00 USD Received 2 Jun 2010; revised 15 Jul 2010; accepted 16 Jul 2010; published 22 Jul 2010